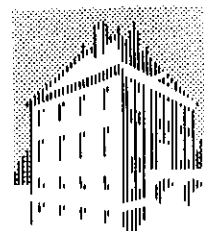


SEPTEMBER 1994

---

FOM-INSTITUUT  
VOOR  
PLASMAFYSICA  
RIJNHUIZEN



ASSOCIATIE  
EURATOM-FOM

---

# MHD STABILITY OF ADVANCED TOKAMAK SCENARIOS

H.A. HOLTIES, G.T.A. HUYSMANS, J.P. GOEDBLOED,  
W.O.K. KERNER, F. SÖLDNER, V. PARAIL

RIJNHUIZEN REPORT 94-221

This work was performed as part of the research programme of the association agreement of Euratom and the 'Stichting voor Fundamenteel Onderzoek der Materie' (FOM) with financial support from the 'Nederlandse Organisatie voor Wetenschappelijk Onderzoek' (NWO) and Euratom.

POSTBUS 1207  
3430 BE NIEUWEGEIN  
NEDERLAND  
EDISONBAAN 14  
3439 MN NIEUWEGEIN  
TEL. 03402 - 31224  
TELEFAX 03402 - 31204

---

# Contents

<b>1</b>	<b>Introduction.</b>	<b>1</b>
<b>2</b>	<b>The infernal mode.</b>	<b>3</b>
<b>3</b>	<b>Model.</b>	<b>4</b>
<b>4</b>	<b>Results.</b>	<b>6</b>
4.1	The reference equilibrium. . . . .	6
4.2	Pressure profile effects. . . . .	8
4.3	Increasing the local current density. . . . .	9
4.4	A broader local current density. . . . .	11
4.5	An optimised equilibrium. . . . .	11
<b>5</b>	<b>Conclusions.</b>	<b>12</b>



## Abstract

We have performed a numerical parameter study in order to find MHD stable operating regimes for advanced tokamak experiments. In this study we have concentrated on internal modes. Ballooning stability and stability with respect to infernal modes are considered. Our calculations confirm that pressure gradients are the main driving force for infernal modes. It is possible to stabilise infernal modes by elimination of pressure gradients in the region of small shear. In the type of equilibrium considered a flat or slightly non monotonic  $q$  profile is most unstable against infernal modes. Higher shear around the minimum  $q$  surface stabilises these modes. Resistivity does not lead to a significant more unstable situation. In the region of positive shear pressure gradients are limited by the destabilisation of ballooning modes. The results of the study have been used to construct an equilibrium that is stable up to  $\beta_p = 3.59$ ,  $\beta_N = 5.44$ .

# 1 Introduction.

In the 1994/1995 experimental campaign at JET, part of the experiments were devoted to creating plasmas with inverted  $q$  profiles commonly encountered in steady state plasmas with a high bootstrap fraction. Current drive and heating mechanisms are used to control the shape of equilibrium profiles, in order to maintain a stable plasma at all times [1]. In this paper the MHD stability study of such scenarios is presented. Because of the general nature of the study the results will also be valid for experiments other than the JET experiment.

In this section we will give an overview of MHD stability considerations for equilibria with inverted  $q$  profiles. Section 2 will present aspects of the infernal mode, a dangerous instability that only exists in plasmas with a low shear region. In section 3 we describe the model used to study the stability for a class of equilibria with inverted  $q$  profiles. Section 4 presents the results of this study, and the conclusions can be found in section 5.

In tokamak fusion research there are two paths being followed which should lead to a working fusion reactor. One path, the one taken by ITER EDA [2], extrapolates experimental results from existing tokamaks. This leads to large machines that have large plasma currents and a pulsed operation. Other approaches, commonly referred to as advanced tokamak scenarios, try to find ways to operate the fusion tokamak in steady state [3, 4, 5]. The advanced tokamak experiments must have their current driven non inductively. From an economic point of view it is advantageous to have a large fraction of the current driven by the bootstrap effect. The bootstrap current is proportional to the pressure gradient:

$$J_{BS} \propto -\sqrt{\epsilon} \frac{\partial p / \partial r}{B_p} , \quad (1)$$

where  $p$  is the pressure,  $r$  a radial coordinate,  $\epsilon$  the local inverse aspect ratio  $r/R$ , and  $B_p$  the poloidal magnetic field. It is clear from this equation, that in order to have a large bootstrap current large values of the poloidal beta are required. Since the pressure gradient has a maximum somewhere off axis it can also be seen that the current profiles of advanced tokamak scenarios will in general be non-monotonic. The non-monotonic current profiles give rise to inverted safety factor profiles which have a minimum that is situated

just outside the position of maximum current. The safety factor  $q$  is defined by:

$$q = \frac{1}{2\pi} \oint \frac{B_\phi}{RB_p} dl, \quad (2)$$

where  $B_\phi$  is the toroidal magnetic field and  $R$  is the major radius. The integral is taken over a single poloidal loop around the flux surface. The shear is given by:

$$s = \frac{\Psi}{q} \frac{dq}{d\Psi}, \quad (3)$$

where  $\Psi$  is the poloidal flux. In the region of small shear around a minimum in the  $q$  profile the so-called infernal mode can become unstable. The infernal mode is a pressure driven internal MHD-instability with low to intermediate toroidal and poloidal mode numbers  $(n, m)$  that is excited in a region of low shear. Several authors [6, 7] have already shown that this infernal mode is easily destabilised and could very well be responsible for limiting the maximum attainable plasma beta. However, still much is to be learned about the exact dependence of the infernal mode on plasma profiles and therefore this mode will be studied in more detail. The MHD stability of the advanced tokamak scenarios requires control of the plasma profiles. To find how these profiles influences the stability is the main objective of this paper.

Apart from the infernal mode there are several types of MHD instabilities that one can expect in the scenarios that we are considering. At first there is the ballooning stability. Ballooning instabilities are high  $n$  pressure driven modes. It is known that negative shear, as well as large positive shear, has a stabilising effect on the ballooning mode, so that we can expect that the plasma region inside the minimum in the  $q$  profile will be able to sustain large pressure gradients before the ballooning mode is destabilised. However, just outside the minimum there is a region of small positive shear which will be the region where ballooning instabilities will limit the pressure gradient the most.

The internal kink mode will not be dangerous because the equilibria are studied in a regime where the minimum value of the safety factor is well above 1. The external kink, on the other hand, could have an influence on the stability boundaries. This is a low- $n$  mode which is mainly driven by a finite edge current density. The stability of this mode has been studied

extensively and much is known about its stability. For example, shaping of the plasma can stabilise the external kink and also large shear at the plasma edge has a stabilising effect. Here, we have used an up-down symmetric D-shaped plasma. This may not be the best shape when external kinks are considered. Plasmas with X-points for example are known to be more stable against kink modes [8]. The external kink has also been studied for plasmas with reversed shear [9, 10, 11]. The pressure driven external kink was found to be dangerous, especially when it couples to internal harmonics in the low shear region. However, our first interest is the infernal mode and we concentrate on this internal instability. The shape of the plasma might not have a big influence on its stability and we have used a simpler shape to make the calculations not unnecessarily time consuming.

## 2 The infernal mode.

The infernal mode is first mentioned in an article by Manickam *et al* [6] where it is shown that in regions of low shear the standard ballooning theory breaks down and it is not necessarily true anymore that the most unstable ballooning type mode is a high- $n$  mode. Instead, if one plots the growth rate as a function of  $nq$  at low  $nq$  an oscillatory behaviour can be seen and unstable bands in  $nq$  are formed. If for a given value of the safety factor  $q$  an integer value of  $n$  coincides with such a window there exists an unstable low  $n$  mode that is called the infernal mode. In reference [6] only monotonic  $q$  profiles were considered.

In 1993 an article was published by Ozeki *et al* [7] in which non-monotonic profiles were taken into consideration. Here it was shown that for the internal low- $n$  MHD stability, and in particular for the infernal mode, a hollow current profile, as compared with parabolic and flat profiles, gives rise to the most unstable equilibrium. Moreover, they showed that for such profiles the infernal mode is the first to be destabilised at high  $\beta_p$  over a large range in parameter space. They also showed that using a more peaked pressure profile could stabilise the infernal instability by moving the maximum pressure gradient out of the region of small shear.

The article of Ozeki *et al* was motivated by the observation of a  $\beta_p$  collapse in JT-60 experiments with a large bootstrap fraction [12]. Also from JET there is evidence that the infernal mode is responsible for a collapse of

the plasma temperature in some pellet fuelled discharges. Here it has been observed [13] that when the safety factor on axis reaches a value of 1.5 the central temperature profile flattens abruptly and a residual  $m = 3$  structure is present afterwards. Charlton *et al* [14] analysed these discharges. They found that for a reconstructed equilibrium the  $q$  profile was flat in the centre and the  $n = 2, m = 3$  infernal mode was unstable for values of  $q_0$  just below 1.5. The calculated growth rate of this instability was in good agreement with the experimentally observed one. From a non-linear time evolution of this mode they also found that its effect on the plasma parameters was to flatten the central pressure profile, just as was observed in the experiment.

More recently work has been done to find stable high  $\beta$  advanced tokamak scenario equilibria for JT-60U [15], DIII-D [16, 17], and for TPX [10, 11]. In these studies self consistent equilibria with a high fraction of the current driven by the bootstrap effect are considered. Also the effect of an external vacuum was taken into account, and found to have a destabilising effect, wall stabilisation was needed in most of the high  $\beta$  calculations. MHD stable equilibria with  $\beta_N$  values above 5 were found in all of these studies.  $\beta_N$  is the normalised beta defined by

$$\beta_N = \langle \beta \rangle / \frac{I_p(\text{MA})}{a(\text{m})B(\text{T})}. \quad (4)$$

$\langle \beta \rangle$  is the volume averaged plasma beta,  $I_p$  is the total plasma current,  $a$  is the minor radius of the plasma, and  $B$  is the vacuum magnetic field on axis.

From all this we can conclude that, although the infernal mode has become of interest only recently, it is a dangerous mode that could very well be one of grave importance to the newly developed advanced tokamak scenarios. We will present an extensive study of the infernal mode stability for plasmas with regions of negative shear in the framework of linear resistive MHD.

### 3 Model.

For the study of the MHD stability of advanced tokamak scenarios three numerical codes have been used. For the construction of MHD equilibria using a pressure gradient profile and a current profile as input the HBT [18, 19] and HELENA [20] codes were used. For this purpose they were extended so as to be able to use an averaged toroidal current density profile as input

for the equilibrium construction. The ballooning stability of these equilibria was calculated with HBT. For the low- $n$  MHD stability the resistive MHD code CASTOR [21, 22] was used. The MHD equilibrium code HELENA was used to calculate the geometric quantities needed by CASTOR.

We have used a JET relevant geometry consisting of a D-shaped plasma with an inverse aspect ratio of 0.34. (The shape of the plasma can be inferred from the outer contour of figure 16.) The constructed equilibria all have a total toroidal plasma current of 2.1 MA but in the parameter studies we will vary the safety factor on axis and the  $q$  profile and plasma current will change accordingly. Low values are taken for the current because it must be driven non-inductively. In most of the stability calculations we have used an ideally conducting wall at the plasma boundary. The equilibrium profiles are parametrised to be able to control important features like the position of the maximum pressure gradient and of the maximum current density. The input profiles are:

$$\langle J_\phi \rangle = \left(1 + A_J \Psi + B_J \Psi^2 + C_J \Psi^3\right)^\alpha + D_J \left(\Psi - \Psi^2\right)^\gamma \exp\left(-((\Psi - \Psi_0)/\delta)^2\right), \quad (5)$$

$$\frac{dP}{d\Psi} = (1 - \Psi)^\lambda. \quad (6)$$

Here  $\langle J_\phi \rangle$  is the flux surface averaged toroidal current density normalised to 1 at the magnetic axis,  $P$  is the plasma pressure, its gradient is also normalised to 1 at the axis, and  $\Psi$  is the normalised flux going from 0 at the axis to 1 at the plasma boundary.

The expression for the toroidal current density consists of two parts. The first part is a power of a truncated series expansion in  $\Psi$  which models the bulk background plasma current. The second part gives locally a bump in the profile of which the position, width, and height can be controlled by respectively  $\Psi_0$ ,  $\delta$ , and  $D_J$ . The function in front of the exponent guarantees that this term will not contribute to the current density on axis and at the edge.  $\gamma$  is a parameter that controls how fast it will go to zero at those positions. The bump gives us control over the position, width, and depth of the local minimum in the  $q$  profile and models a locally driven current coming either from bootstrap effects (which we did not take into account self-consistently) or from an external mechanism like lower hybrid current

drive. The pressure gradient profile consists of a power of  $(1 - \Psi)$ . In the part of this paper where local pressure gradient effects are studied a function of the form

$$\begin{aligned}
\Psi < \Psi_c - \Delta & : f(\Psi) = 0, \\
\Psi_c - \Delta \leq \Psi < \Psi_c & : f(\Psi) = -f_0 (\Psi - (\Psi_c - \Delta))^2 (2\Psi_c + \Delta - 2\Psi), \\
\Psi_c \leq \Psi \leq \Psi_c + \Delta & : f(\Psi) = -f_0 (\Psi - (\Psi_c + \Delta))^2 (2\Psi_c - \Delta - 2\Psi), \\
\Psi_c + \Delta < \Psi & : f(\Psi) = 0
\end{aligned} \tag{7}$$

is added to the pressure gradient profile. This gives rise to a localised change in the pressure profile around  $\Psi_c$  with width  $2\Delta$  and amplitude  $f_0$ . These parametrisations leave us enough freedom to study a wide range of profile effects on the stability.

## 4 Results.

In this section we will look at the dependence of the infernal instability on several parameters. First, we will look at the stability of a reference equilibrium which was chosen to resemble typical equilibria produced by the transport code JETTO [23] in the modelling phase of the profile control experiments at JET. After this we will look at the effects of changes in the pressure and the current profile.

### 4.1 The reference equilibrium.

We start studying the effects of equilibrium parameters on the stability of equilibria with a region of negative shear. In this section we look at a reference equilibrium that will be used as a starting point for the remainder of the paper. The pressure profile, the current density profile and the safety factor profile of this equilibrium are shown in figure 1. The pressure gradient is largest halfway between the magnetic axis and the plasma edge, not far from the region of small negative shear. The edge safety factor is high. This is caused by the low plasma currents that are used in the profile control experiments.

As has been noted in [7],  $q_{min}$  is a very important parameter for the stability of the infernal mode. The infernal mode is most unstable for values

of  $q_{min}$  just below a rational value so that there are two resonant surfaces in the plasma and the infernal mode is mainly localised between these two surfaces, or there is a large low shear region extending up to, and including, the plasma centre where infernal modes can be excited. As could have been expected from the analysis by Manickam *et al* [6] the growth rate is a function of  $n$  times  $q$  rather than of the safety factor alone so that for higher values of  $n$  the range of unstable  $q$  values is smaller, but successive unstable regions are closer together. Figure 2 shows the critical value of  $\beta_p$  above which infernal modes become unstable plotted against  $q_{min}$  for  $n = 1, 2,$  and  $3$ . (Only the most unstable mode number is shown.). In this scan all profiles for a given  $\beta_p$  are kept fixed, while the total current is varied. The  $q$  profile scales approximately with the inverse of the total current. For  $\beta_p = 1.75$  the  $q_{min}$  value corresponding to a total current of 2.1 MA is 1.56. From this figure one can also see the strong destabilisation at high current (low  $q$ ).

Infernal modes are pressure driven instabilities. Figure 3 shows the growth rate of the infernal mode against  $q_{min}$  of the reference equilibrium for three values of  $\beta_p$ . The growth rate is normalised to the inverse of  $\tau_A$ ,  $\tau_A = R_m/V_A$ ,  $R_m$  is the major radius of the magnetic axis, and  $V_A$  is the Alfvén speed on the magnetic axis. There exists a critical value of  $\beta_p$  below which the equilibrium is stable against infernal modes. The critical value below which the  $n = 1$  mode around  $q_{min}$  becomes stable in this equilibrium is 1.41. It is stable against ballooning modes for  $\beta_p$  smaller than 1.44. At low  $\beta_p$  the infernal mode can be stabilised. This fact can be utilised in the start-up phase of an experiment to fix the profiles at low  $\beta$  and start heating while keeping the profiles (in particular the  $q$  profile) constant. In this way dangerous parameter regimes for the infernal instability can be avoided. The dependence of stability on the pressure gradient will be studied in more detail in section 4.2.

In figure 4 we can see the effect that resistivity has on the infernal mode. Here  $\eta$  is the resistivity normalised with respect to  $\mu_0 V_A R_m$ , where  $\mu_0$  is the magnetic permeability. Resistivity has the strongest influence on stability on the low  $q$  side where the infernal mode develops steep gradients that are stabilising for ideal modes, but that get smoothed out by the inclusion of resistivity. Finite values of the resistivity destabilise the infernal mode for parameter ranges where the ideal case is stable. However for realistic values of the resistivity (in JET this would mean  $\eta \approx 10^{-8} - 10^{-9}$ ) there is no significant effect on the stability boundary. It seems that no new more

unstable mode develops, resistivity just alters the ideal mode. This resistive infernal mode could be related to double tearing modes.

The fixed boundary used almost everywhere in this paper has, at low  $q$  values, a strongly stabilising effect. Using a wall at a distance of twice the plasma radius shows that the  $n = 1$  infernal mode becomes unstable for all values of  $q_{min}$  smaller than 2 (figure 5). The critical value of  $q_{min}$  on the high side does not change significantly. The marginally stable infernal mode at this value of  $q$  is highly localised in the zero shear region and does not feel the effect of a free boundary. The conclusion must be that care should be taken not to create a zero shear region close to the plasma boundary. From now on we will concentrate on the effect of equilibrium profiles, using a fixed boundary. Unless specified otherwise  $\beta_p$  equals 1.75 for these equilibria.

## 4.2 Pressure profile effects.

In figure 6 three equilibrium pressure profiles are shown. The current density profile is identical to the one in figure 1. Profile B belongs to the reference equilibrium. Subtle changes in the pressure profile can already have a significant effect on the stability of infernal modes, while that of ballooning modes hardly changes at all. (For the profiles shown the ballooning critical  $\beta_p$  changes from 1.43 to 1.47.) This seems to be because the pressure gradient changes most in the region of zero shear, while ballooning modes are first destabilised in a region of small but finite positive shear around  $s = 0.62$ . The ballooning calculations are done keeping the pressure and current profiles constant, while varying their relative amplitude such that the total current remained constant and only the plasma beta changed. In the central region of the plasma we have a negative shear, and here the plasma enters a second region of stability. As long as a the large pressure gradient is localised inside the minimum in  $q$ , high values of plasma pressure, and thus of the plasma beta, can be reached.

The infernal mode is destabilised by a pressure gradient in the region of small shear. The shear on the outside of the minimum in  $q$  is higher than on the inside and this has a stabilising effect on the infernal mode when the maximum pressure gradient is located there.

As Ozeki *et al* [7] have shown, moving the largest pressure gradient to the inside also is stabilising for infernal modes. The pressure profile of an optimal equilibrium will be a trade-off between ballooning and infernal stability con-

siderations, and the fact that for pressure profiles peaked in the centre large values of the central pressure are needed to get a significant improvement of the plasma averaged beta compared to a configuration with a broad pressure profile.

The effect of the pressure gradient in the low shear region becomes more clear when we flatten the pressure profile locally. In fig. 8 equilibrium A corresponds to the reference equilibrium. Profiles A, B, and C have a finite gradient everywhere. In figure 9 the stability curves for these equilibria are shown. Increasing the amplitude of the local change such that the pressure gradient is zero on the shearless surface (equilibrium D in figure 8) makes that the infernal mode becomes stable for  $\beta_p$  smaller than 1.76. One can conclude that local effects can stabilise infernal modes.

As a further check that it is not the complete pressure profile from the low shear region inward that drives the modes unstable figure 10 shows three equilibria where the pressure gradient is removed in the centre of the plasma up to some radius. Here  $\beta_p$  for equilibrium A equals 1.75 while for the other equilibria  $\beta_p$  is chosen such that the pressure profile on the outside of the plasma is identical to that of equilibrium A. In this way we can separate the localised effect on the inside from global changes in the pressure profile. From the stability curves (figure 11) we conclude that only when the zero gradient region extends up to the plasma region where the infernal mode has a large amplitude it causes a stabilisation. That is, the gradient change must extend to approximately within the two rational q surfaces. Therefore, the effect is first seen on the low  $q_{min}$  side, while the overall stability limit does not change much.

The dependence on the pressure gradient in the low shear region indicates that infernal modes might have a self healing character. The infernal modes encountered in this study are similar to interchange modes (see fig. 16). This means that neighbouring flux surfaces are interchanged by the mode and the plasma profiles have the tendency to be flattened. The infernal mode could thus remove its own driving force and be stabilised without doing too much damage to the global plasma parameters.

### 4.3 Increasing the local current density.

Here we will look at the influence of an increase of the localised bump in the current density relative to the background current density by increasing the

Table I: Plasma betas for which the five equilibria of fig. 12 are marginally stable to infernal and ballooning modes. Also shown are the flux coordinates at which ballooning modes are first destabilised.

profile	$\beta_p$ (infernal)	$\beta_p$ (ballooning)	$\sqrt{\Psi}$
A	1.88	0.84	0.17
B	1.51	1.17	0.51
C	1.40	1.29	0.57
D	1.41	1.44	0.62
E	1.69	1.55	0.65

parameter  $D_J$  in equation 5. The five current and safety factor profiles that are considered here are shown in figure 12. In the figure the current profile is normalised such that for profile D (the reference equilibrium) the current density on axis is equal to one. The value of the safety factor on a given flux surface mainly depends on the total current that flows within this surface. When we increase the localised bump with respect to the background current this means that the current density near the axis diminishes, and this causes an increase in the central  $q$  value. The  $q$  profile changes from monotonic to flat and to non monotonic.

In figure 13 the resulting stability curves for the  $n = 1$  infernal stability of equilibria B, C, D, and E are shown. Equilibrium A is stable against this infernal mode for  $\beta_p = 1.75$ . Table I shows the critical  $\beta_p$  values of the equilibria against the  $n = 1$  infernal mode around  $q = 2$  and against ballooning modes, as well as the  $\sqrt{\Psi}$  value of the flux surface where ballooning modes are first destabilised. It is found that infernal modes are most unstable for a flat or slightly non monotonic  $q$  profile, while ballooning modes are most stable for a strongly non monotonic profile. Furthermore, for the flat profile the values of the critical beta against infernal and ballooning modes are approximately equal. (Note that in most cases the critical value for infernal stability is larger than that for ballooning stability.) For the flat profile the infernal mode ‘senses’ the existence of a localised current, since it becomes most unstable not for  $q_{min}$  ( $= q$  on axis) just below 2, but for a smaller value

such that the  $q = 2$  surface is in the proximity of the region of maximum current density. From the table it can be seen that the flux surface that becomes first unstable against ballooning modes shifts with  $q_{min}$ , such that it is in the region of small but finite positive shear.

#### 4.4 A broader local current density.

In this section we will look at the effect of a broader localised current density. For this purpose we keep the fraction of localised current approximately constant by fixing  $q$  on axis in the formed equilibrium, but concentrating this localised current in a smaller region. In figure 14 the equilibrium profiles are shown. Equilibrium A is the reference equilibrium. The effect is to vary the depth of the well in the  $q$  profile, but in contrast to the previous section this variation is more local and also varies the width of the well, and thereby the shear on the inside and on the outside of the minimum in the safety factor.

The effect on the ballooning stable  $\beta_p$  is minimal. (It changes from 1.44 to 1.41.) There is however a significant effect on the infernal stability as can be seen from figure 15. For case C the critical  $\beta_p$  stable against infernal modes has increased to 1.65. This localising of the current also causes the small shear region to decrease in radial extent so that infernal modes are more localised. This is illustrated in figure 16, where we show vector plots of the infernal modes for cases A and C at  $q_{min} = 1.87$ . For case C the unstable mode extends over a much smaller volume of the plasma. This means that for such a profile the effect of the instability on the plasma is only local and could therefore be less dangerous for the overall confinement.

#### 4.5 An optimised equilibrium.

Now that we have studied equilibrium effects on MHD stability in reversed shear plasmas in considerable detail we will try to find an equilibrium optimised against ballooning and infernal modes. We start with the current density profile encountered in the study so far that was most stable against the combined consideration of infernal and ballooning modes. Since we find that ballooning modes usually pose the most restrictive demands we will optimise the pressure gradient profile against these modes and check afterwards what the stability against infernal modes is. This optimisation only needs

to be done in the region of positive shear since ballooning modes enter the second region of stability in the negative shear region. The resulting profiles are shown in fig. 17. The final pressure profile has a large gradient in the region of negative shear, and a smaller value outside the zero shear surface.

The equilibrium is stable against ballooning modes up to  $\beta_p = 3.59$  ( $\beta_N = 5.44$ ). The big rise in beta compared to the cases studied so far is mainly due to the introduction of a pressure gradient in the outer region of the plasma. The equilibrium is also stable against  $n = 1$  infernal modes around  $q_{min} = 2$ . However it is still unstable against  $n = 2$  modes around  $q_{min} = 1.5$ . The latter modes are much harder to stabilise and become stable only for values of  $\beta_p$  below 2.0. At  $\beta_p = 3.59$  this mode is unstable for  $q_{min} \leq 1.55$ . The results show that it is possible to reach considerable values for the plasma beta, especially when there is sufficient control of the plasma profiles.

## 5 Conclusions.

We have found that a number of plasma parameters are important for the stability.

At first, the infernal mode, because it is pressure driven, is destabilised by a large pressure gradient in the region of small shear. Moving the maximum pressure gradient to the region of large shear near the plasma boundary has a stabilising effect although this can have an undesirable effect on the ballooning stability of the plasma.

Low shear in a large part of the plasma makes infernal modes very dangerous. A large region of small or negative shear is however desirable when ballooning modes are considered. Going to low values of  $q_{min}$  (large current densities) has a destabilising effect on infernal modes. Making the sides of the well in the  $q$  profile steeper has, through the larger shear, an effect that the growth rate of the infernal mode becomes smaller. Having a very localised minimum in the  $q$  profile forces the infernal instability to be localised also. It could turn out (and this should be investigated) that, following the results of reference [14], the infernal mode flattens the pressure profile locally, thereby removing its driving force. In that case, a localised instability might not lead to deterioration of the plasma parameters and this could be acceptable.

A high  $\beta$  stable equilibrium will be characterised by negative shear in the plasma centre, the  $q$  profile reaching a shallow minimum on the outside

of the plasma that extends over a small region and  $q$  growing fast at the edge. The pressure gradient will be limited by stability considerations. It can be large in the core but will have to fall before the  $q$  profile reaches its minimum. In the region of positive shear it will be limited by ballooning stability considerations. It seems unlikely that such plasmas can be obtained without external current drive mechanisms.

Control of the positions of small shear and of high pressure gradients is needed to guarantee MHD stability. In the start-up phase of an advanced tokamak experiment, low beta plasmas could be used to prepare a current profile (and thereby a desirable  $q$  profile), and when this profile is reached, to try to freeze it in with external current drive mechanisms while heating the plasma to obtain high beta values. In this way dangerous regimes with a low shear region extending over much of the plasma can be overcome, and a MHD stable route to high  $\beta$  plasmas with a high bootstrap fraction and reversed shear can be found.

## Acknowledgement.

This work was performed as part of the research programme of the association agreement of Euratom and the 'Stichting voor Fundamenteel Onderzoek der Materie' (FOM) with financial support from the 'Nederlandse Organisatie voor Wetenschappelijk Onderzoek' (NWO) and Euratom. It was partly funded under JET study contract no. JT3/13761.

## References

- [1] F.X. Söldner *et al*, *Contr. Fusion and Plasma Physics, (Proc. 21st Eur. Conf. Montpellier)* **18B**, Part III (1994) 1126.
- [2] ITER Joint Central Team, *Plasma Phys. Contr. Fus.* **35** (1993) B23.
- [3] M. Kikuchi, *Plasma Phys. Contr. Fus.* **35** (1993) B39.
- [4] R.J. Goldston *et al*, *Contr. Fusion and Plasma Physics, (Proc. 20th Eur. Conf. Lisbon)* **17C**, Part I (1994) 319.
- [5] R.J. Goldston *et al*, *Plasma Phys. Contr. Fus.* **36** (1994) B213.

- [6] J. Manickam, N. Pomphrey, A.M.M. Todd, *Nucl. Fusion* **27** (1987) 1461.
- [7] T. Ozeki, M. Azumi, S. Tokuda, S. Ishida, *Nucl. Fusion* **33** (1993) 1025.
- [8] T. Ozeki, M. Azumi, H. Ninomiya, S. Tokuda, T. Tsunematsu, S. Seki, *Nucl. Fusion* **28** (1988) 1859.
- [9] J. Manickam, in *Workshop on Stabilization of the external kink and other MHD issues*, June 23-25, 1993, San Diego.
- [10] C. Kessel, J. Manickam, G. Rewoldt, W.M. Tang, *Phys. Rev. Lett.* **72** (1994) 1212.
- [11] J. Manickam, M.S. Chance, S.C. Jardin, C. Kessel, D. Monticello, N. Pomphrey, A. Reiman, C. Wang, L.E. Zakharov, *Phys. Plasmas* **1** (1994) 1601.
- [12] S. Ishida, Y. Koide, T. Ozeki, M. Kikuchi, S. Tsuji, H. Shirai, O. Naito, M. Azumi, *Phys. Rev. Lett.* **68** (1992) 1531.
- [13] JET Team, in *Plasma Physics and Controlled Nuclear Fusion Research 1988 (Proc. 12th Int. Conf. Nice, 1988)*, **1**, IAEA, Vienna (1989) 215.
- [14] L.A. Charlton, L.R. Baylor, A.W. Edwards, G.W. Hammett, W.A. Houlberg, P. Kupschus, V.E. Lynch, S.L. Milora, J. O'Rourke, G.L. Schmidt, *Nucl. Fusion* **31** (1991) 1835.
- [15] T. Ozeki, M. Azumi, Y. Kamada, S. Ishida, Y. Neyatani, S. Tokuda, *Nucl. Fusion* **35** (1995) 861.
- [16] T.S. Taylor *et al*, *Plasma Phys. Contr. Fus.* **36** (1994) B229.
- [17] A.D. Turnbull, T.S. Taylor, Y.R. Lin-Liu, H. St. John, *Phys. Rev. Lett.* **74** (1995) 718.
- [18] J.P. Goedbloed, *Comp. Phys. Commun.* **24** (1981) 311.

- [19] J.P. Goedbloed, G.M.D. Hogewey, R. Kleiberger, J. Rem, R.M.O. Galvão, P.H. Sakanaka, *Plasma Physics and Controlled Nuclear Fusion Research 1984 (Proc. 10th Int. Conf. London, 1984)*, **2**, IAEA, Vienna (1985) 165.
- [20] G.T.A. Huysmans, J.P. Goedbloed, W. Kerner, *Proc. CP90 Conf. on Comp. Phys. Proc.*, World Scientific Publ. Co. (1991) 371.
- [21] W. Kerner, S. Poedts, J.P. Goedbloed, G.T.A. Huysmans, B. Keegan, E. Schwarz, *Contr. Fusion and Plasma Physics (Proc. 18th Eur. Conf. Berlin)*, **4** (1991) 89.
- [22] G.T.A. Huysmans, J.P. Goedbloed, W. Kerner, *Phys. Fluids B* **5** (1993) 1545.
- [23] G. Cenacchi, A. Taroni, *8th Eur. Conf. on Comp. Phys. Eibsee* (1986).

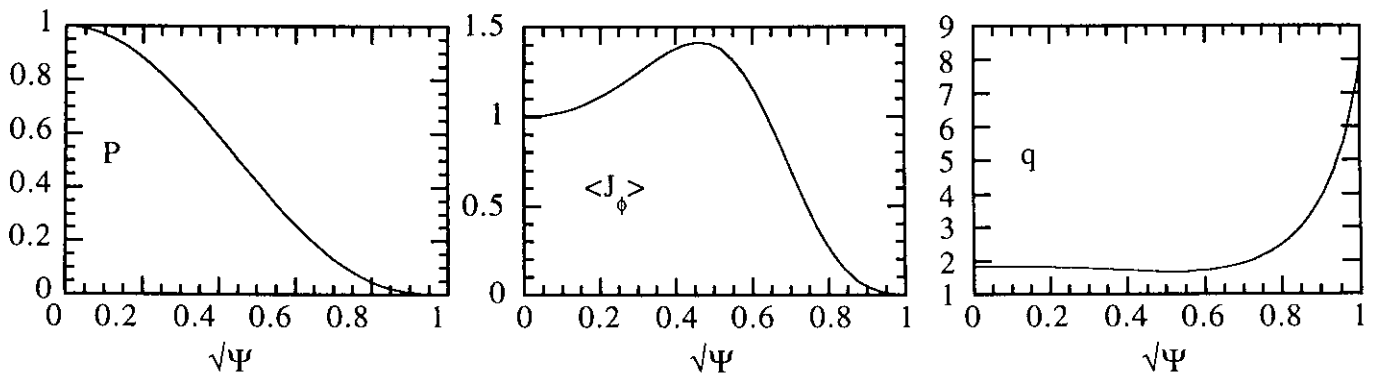


Figure 1: *The pressure, current density, and safety factor profiles of the reference equilibrium. Here  $\Psi$  is the normalised flux.*

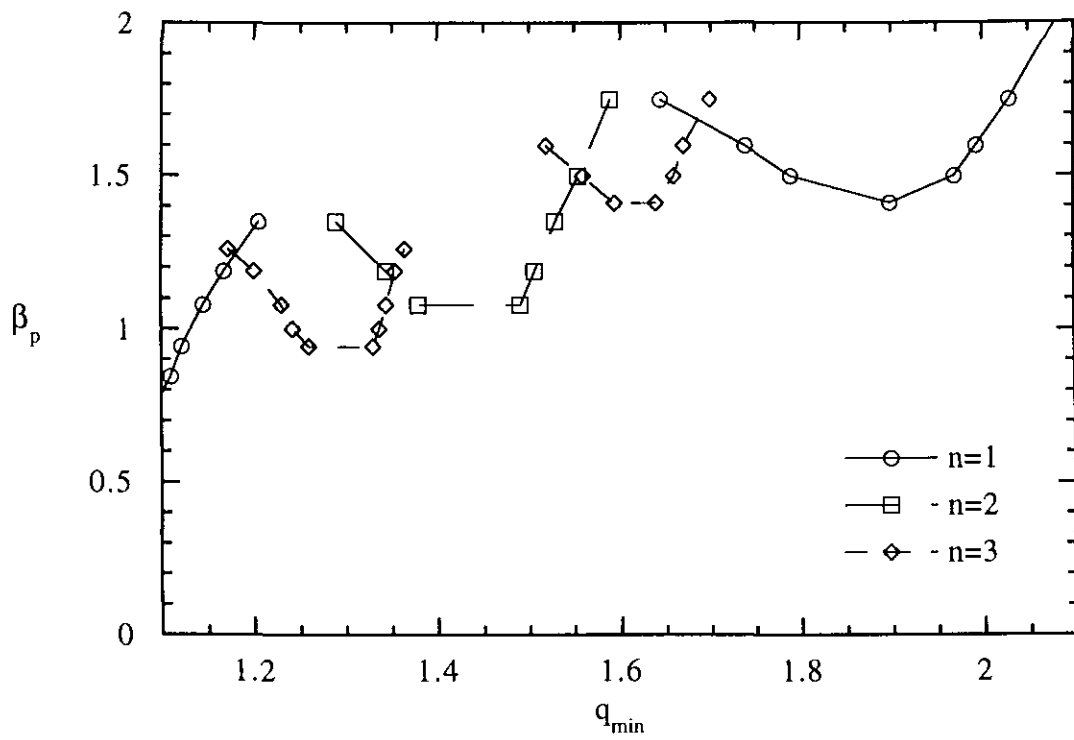


Figure 2: Critical  $\beta_p$  for infernal mode stability as a function of the value of  $q_{\min}$  for the reference equilibrium; Curves are shown for  $n = 1, 2, 3$ .

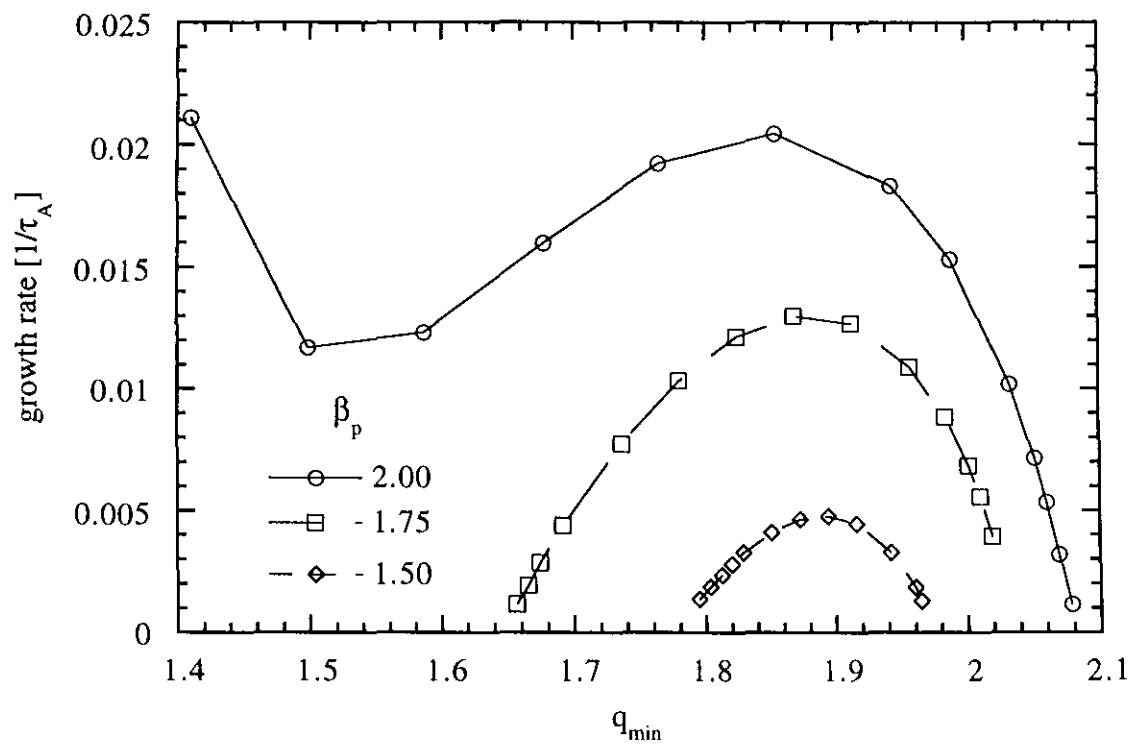


Figure 3: Growth rate of the  $n = 1$  infernal mode for  $\beta_p = 1.5$ , 1.75, 2.0.

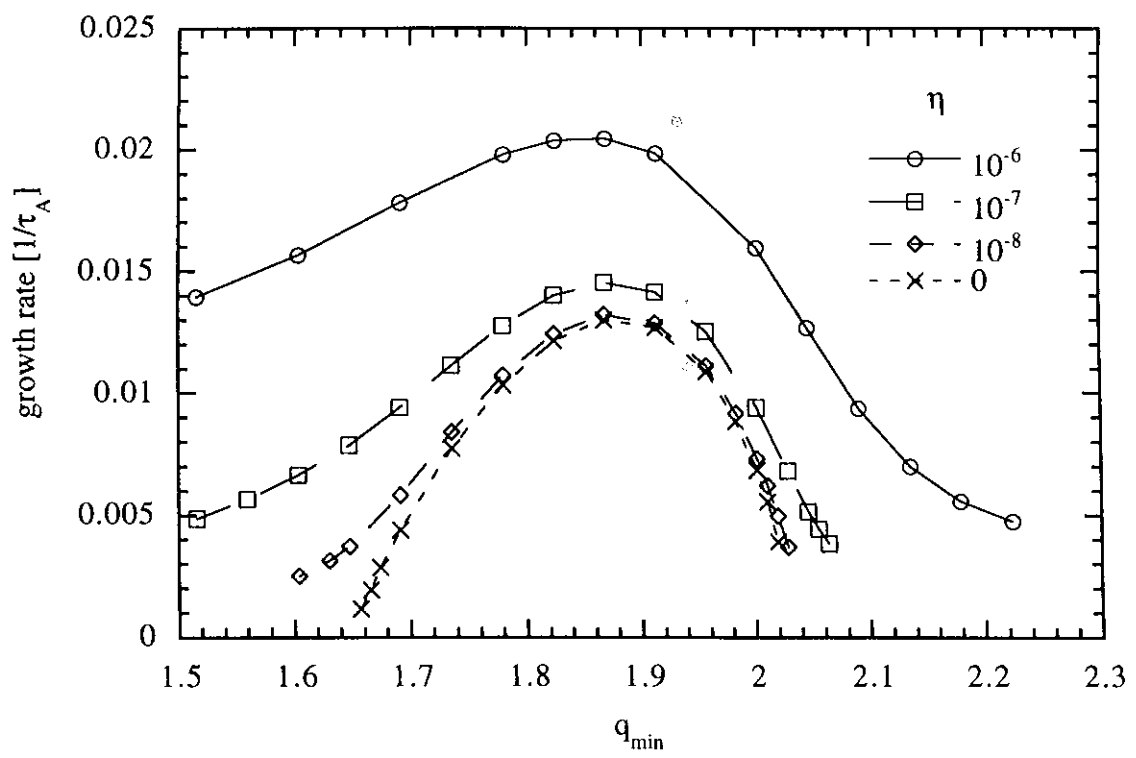


Figure 4: Influence of resistivity on the growth rate of the infernal mode.

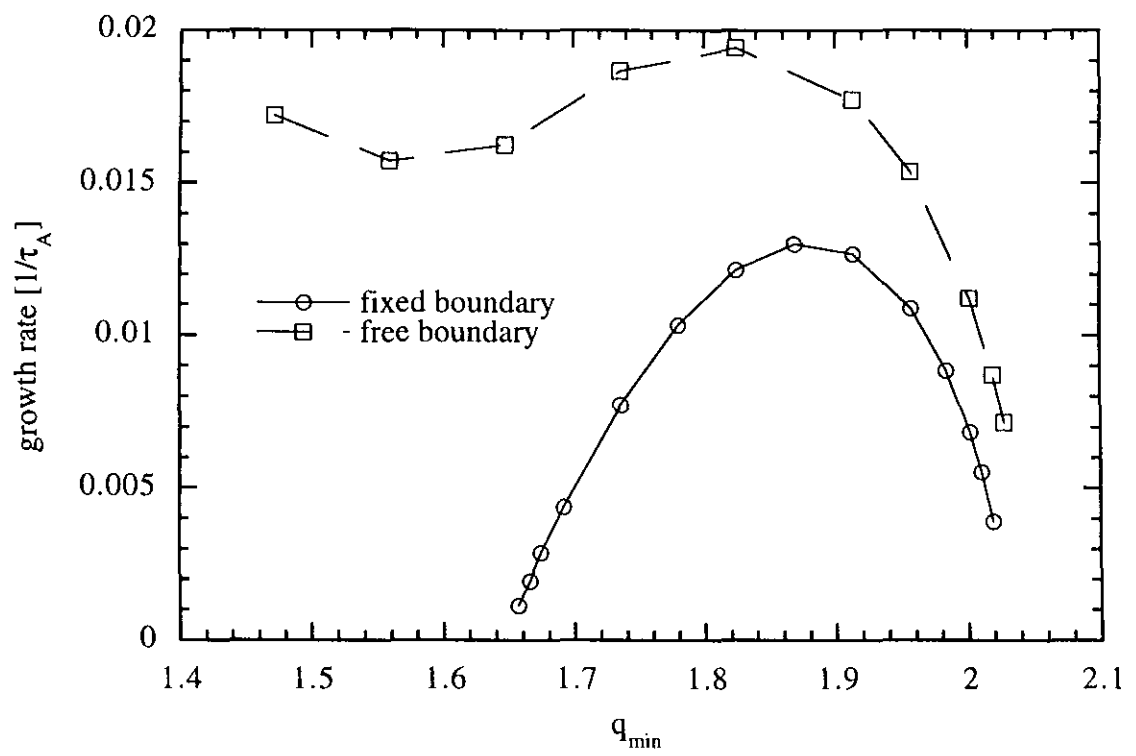


Figure 5: *Influence of a free boundary on the growth rate of the infernal mode.*

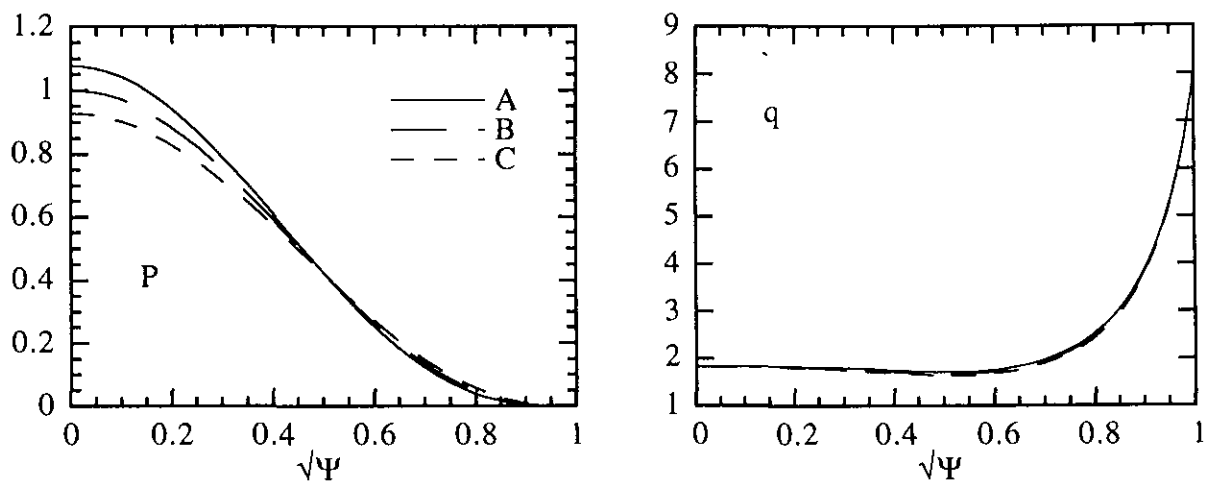


Figure 6: *Pressure and safety factor profiles used to study the dependence of the infernal stability on the overall pressure profile. The current density profile is kept fixed.*

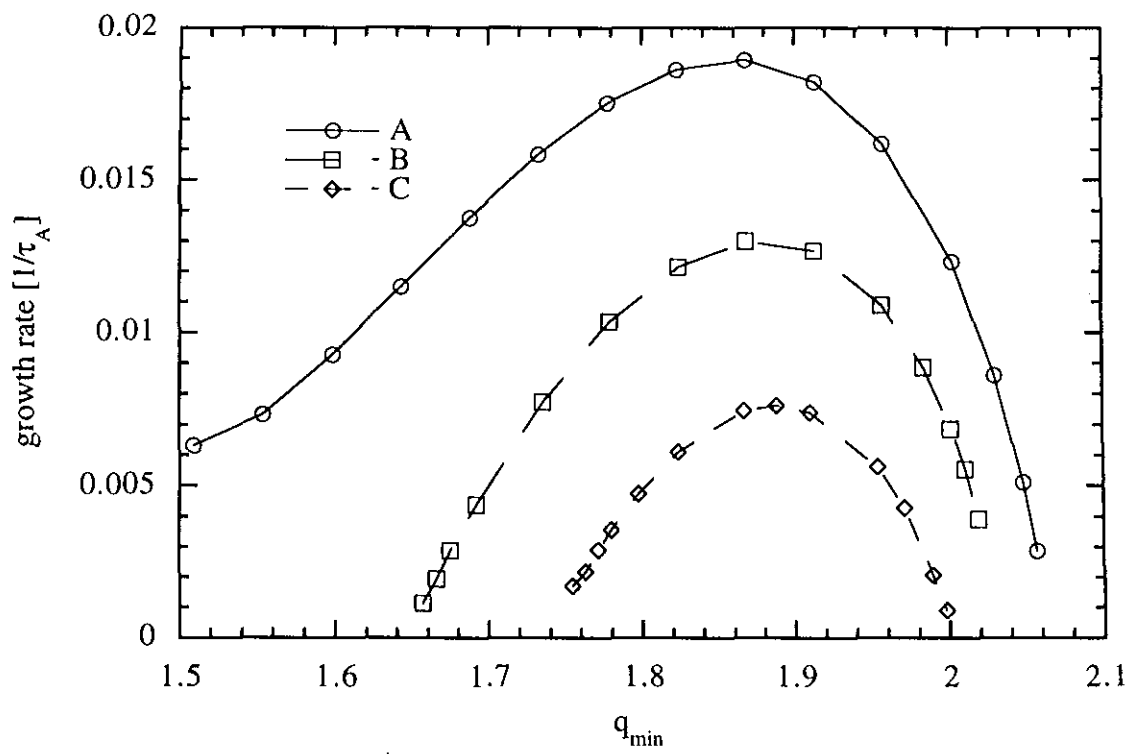


Figure 7: Growth rate of the infernal mode for the three equilibria shown in fig. 6.

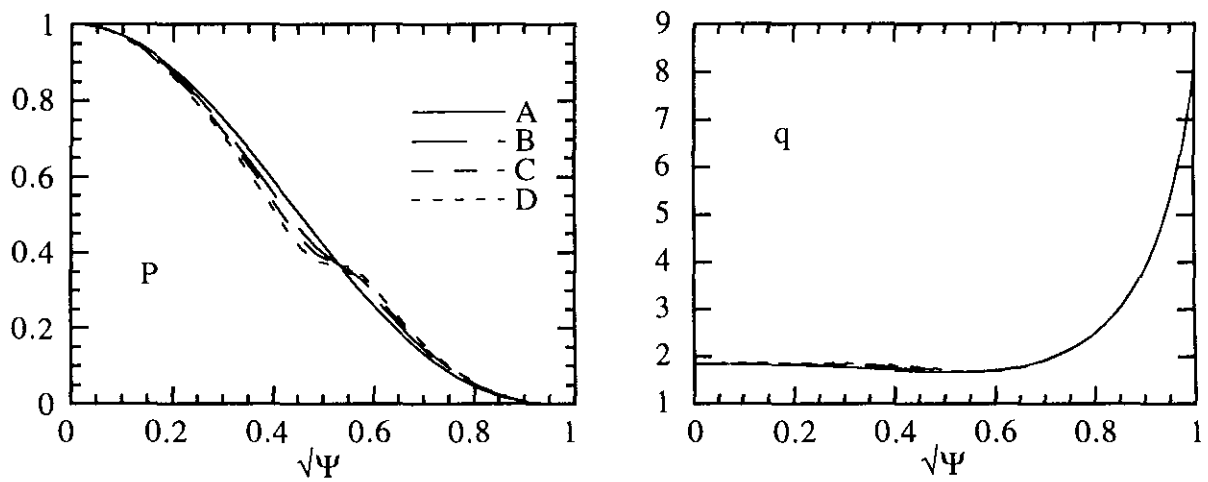


Figure 8: *Pressure and safety factor profiles used to study the dependence of the infernal stability on the local pressure gradient. The current density profile is kept fixed.*

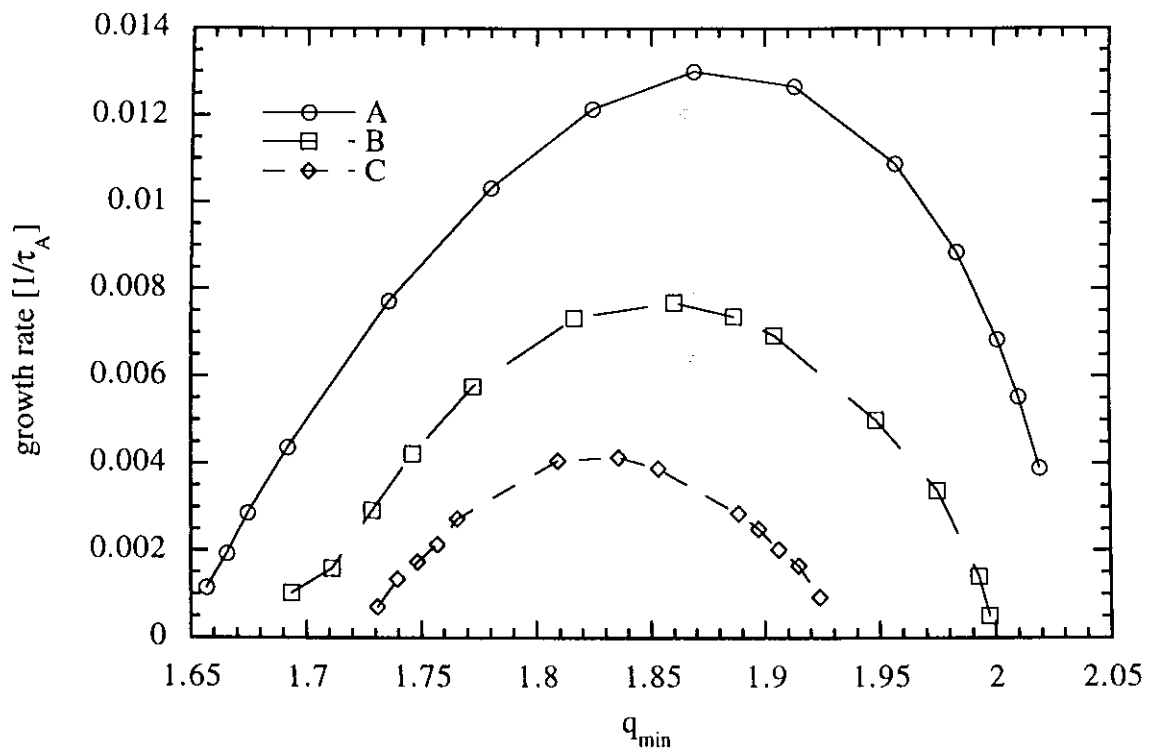


Figure 9: *Growth rate of the infernal mode for the equilibria shown in fig. 8.*

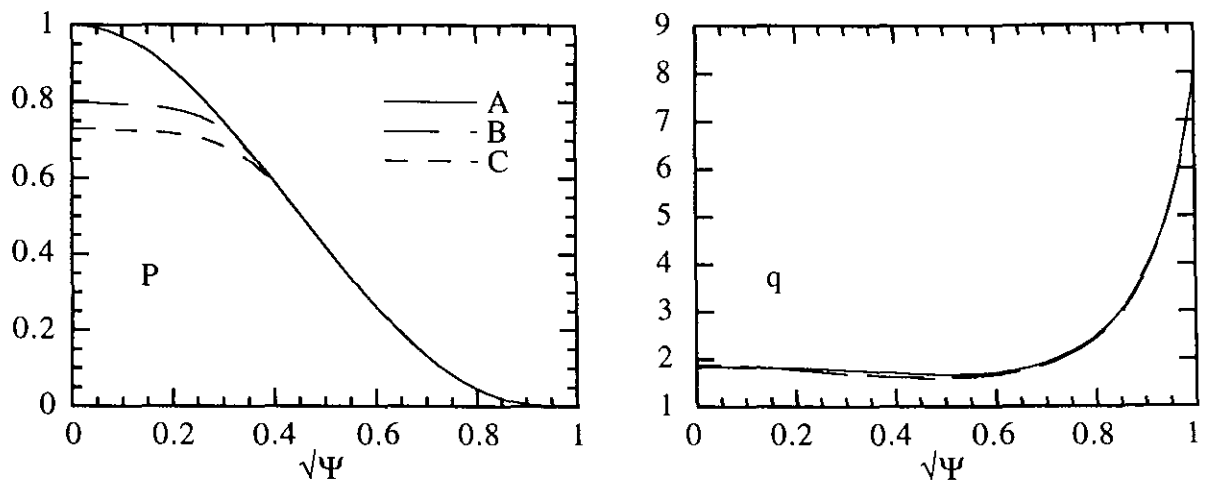


Figure 10: *Pressure and safety factor profiles used to study the dependence of the infernal stability on the pressure gradient near the plasma center. The current density profile is kept fixed.*

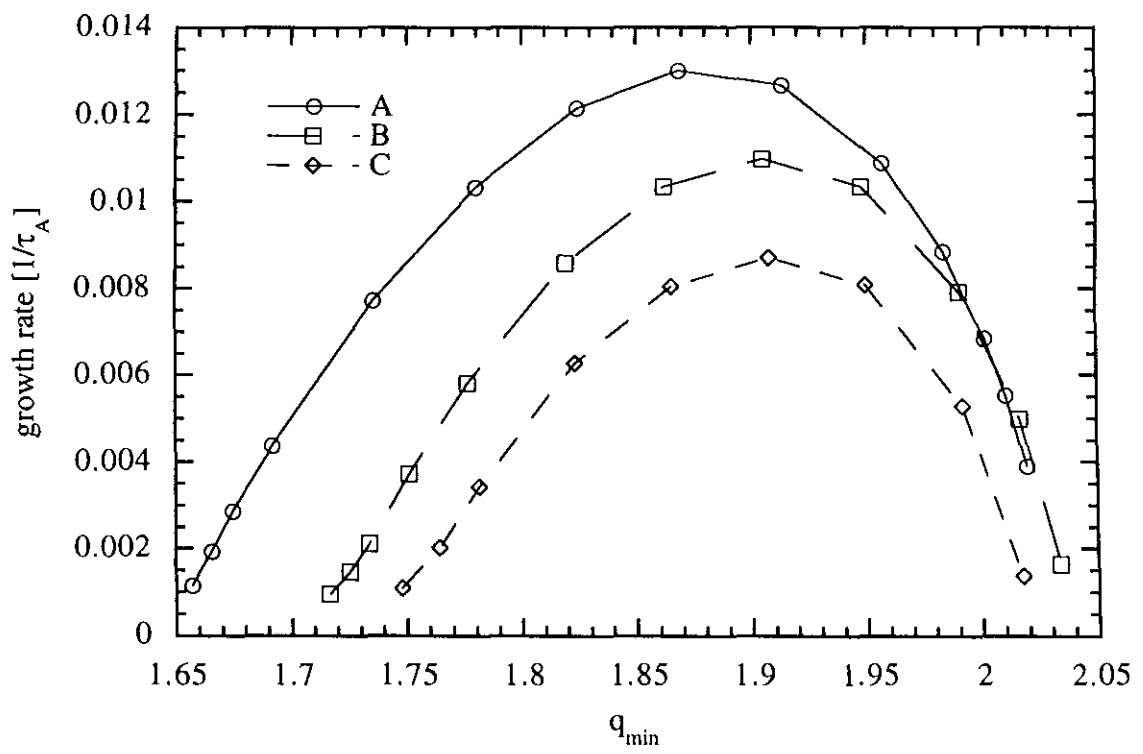


Figure 11: *Growth rate of the infernal mode for the three equilibria shown in fig. 10.*

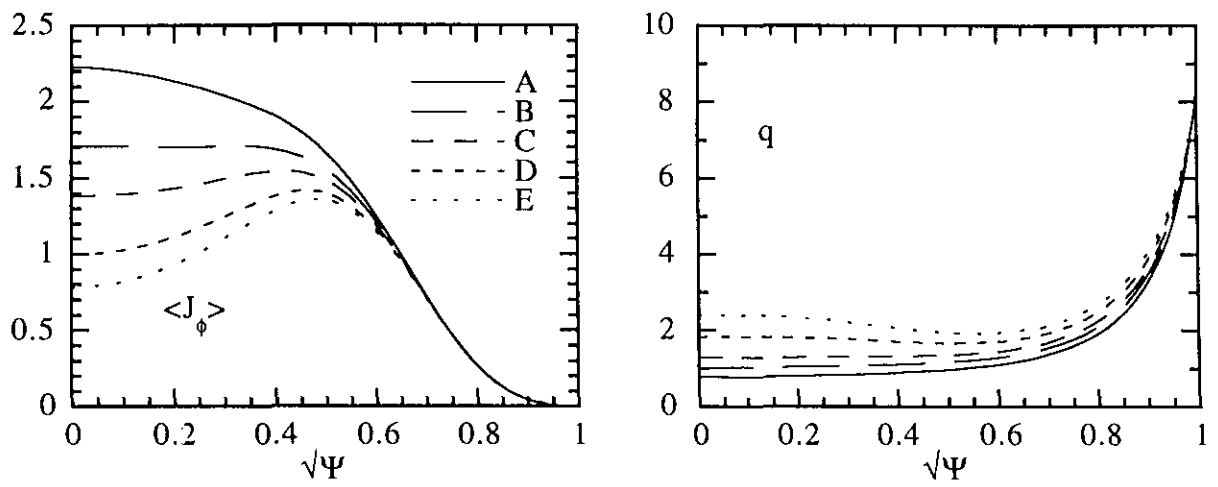


Figure 12: *Current density and safety factor profiles used to study the dependence of the infernal stability on a variation of  $q$  in the plasma centre.*

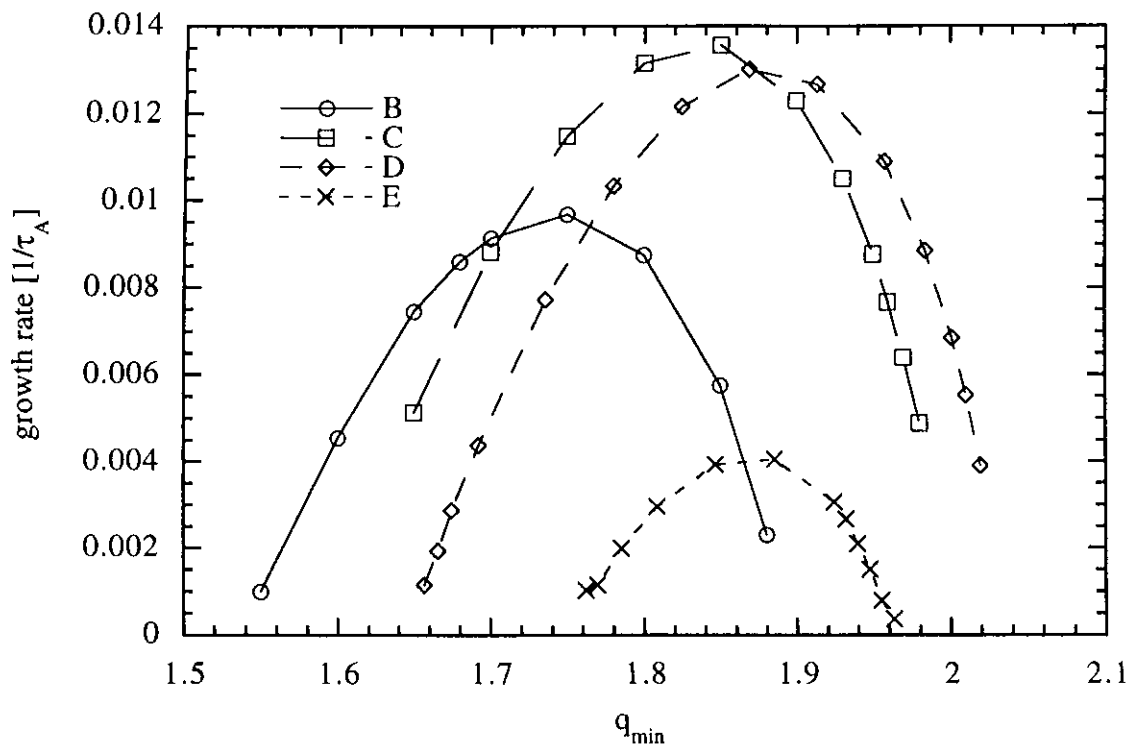


Figure 13: *Growth rates of the infernal mode for the equilibria shown in fig. 12.*

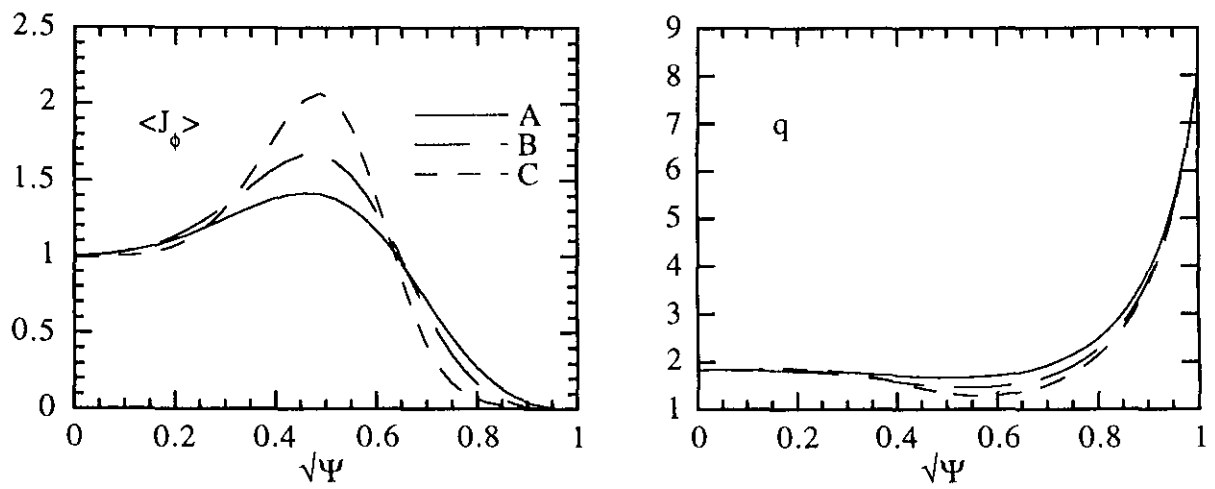


Figure 14: *Current density and safety factor profiles used to study the dependence of the infernal stability on the width of the low shear region.*

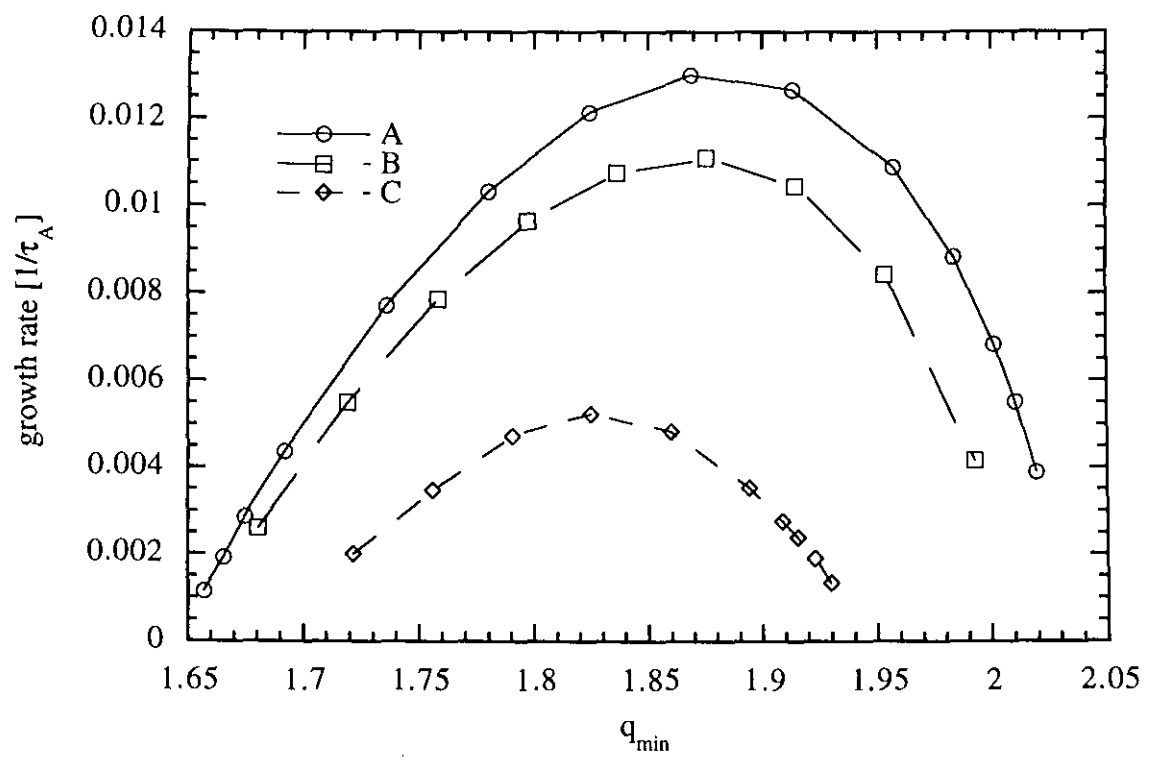


Figure 15: *Growth rates of the infernal mode for the three equilibria shown in fig. 14.*

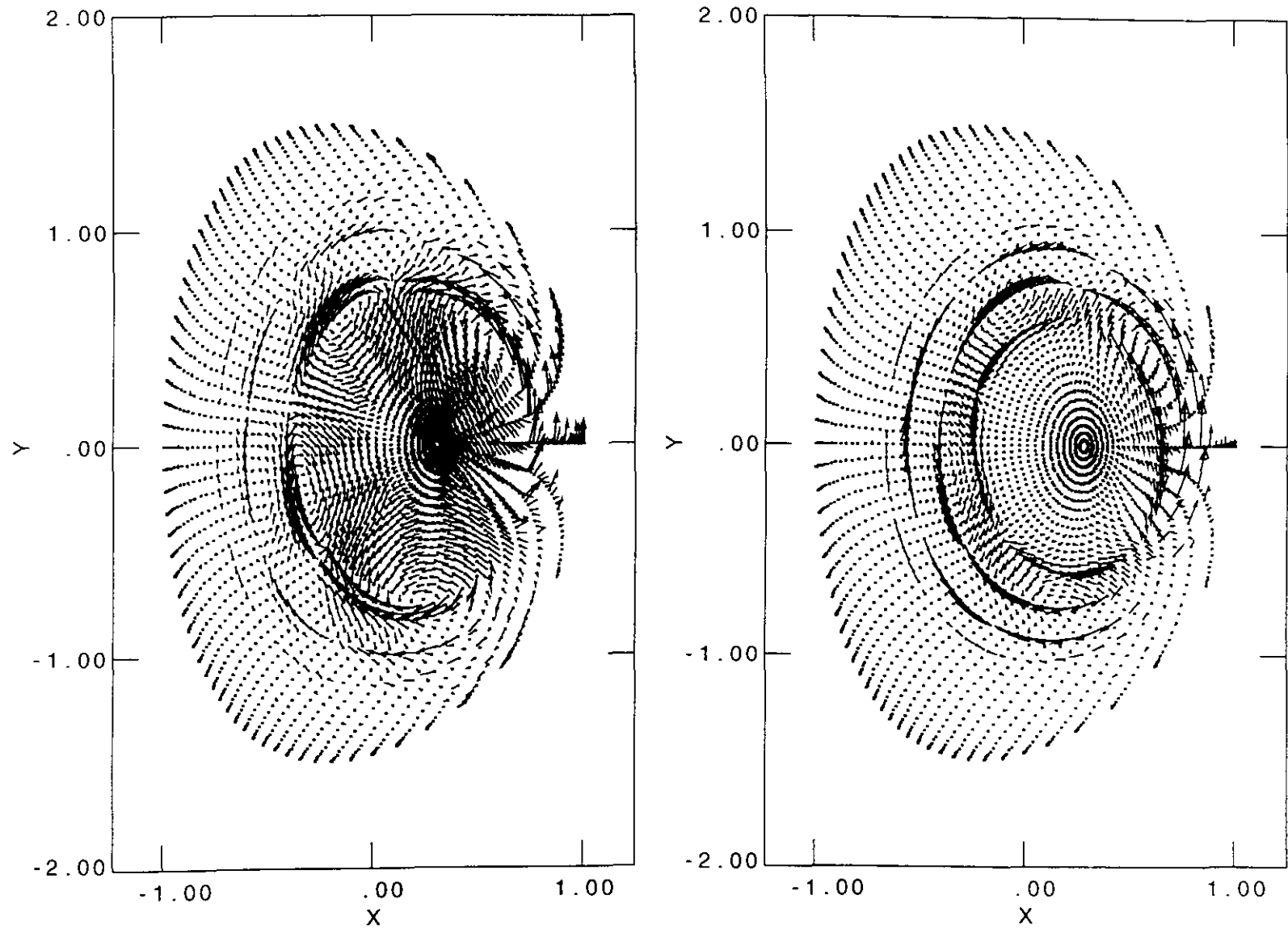


Figure 16: *Vector plots of the infernal mode at  $q_{min} = 1.87$  corresponding to case A (left) and case C (right) of fig. 14. The infernal mode on the left extends over a larger plasma volume.*

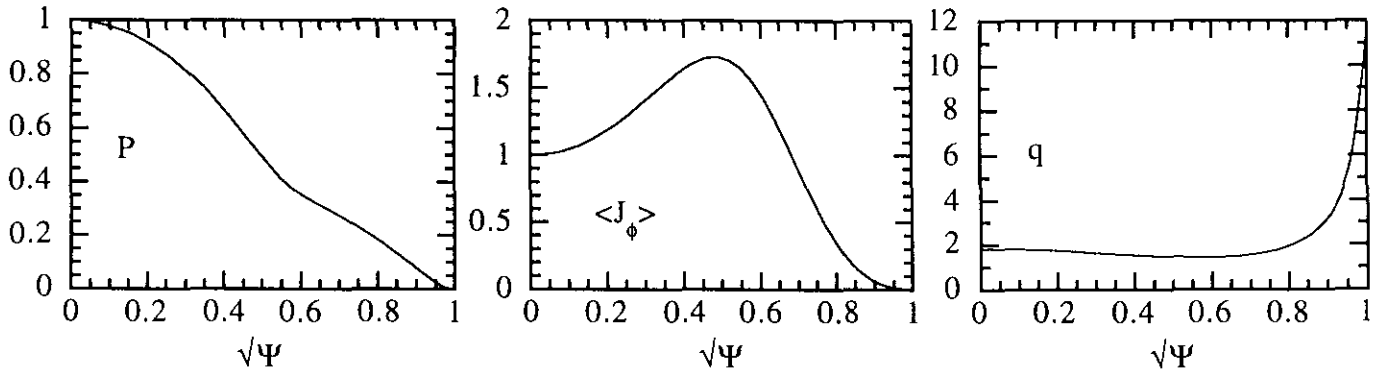


Figure 17: *Pressure, current density and safety factor profile of an equilibrium optimised with respect to internal instabilities.*